Toward Improved Electromagnetic Tracking for Handheld Robotics

R. A. MacLachlan, R. L. Hollis
The Robotics Institute
Carnegie Mellon University
Pittsburgh, Pennsylvania, USA
ram@ri.cmu.edu;
rhollis@ri.cmu.edu

J. N. Martel, L. A. Lobes, Jr.
Dept. of Ophthalmology
University of Pittsburgh
Pittsburgh, Pennsylvania, USA
marteljn@upmc.edu;
lalobes@gmail.com

C. N. Riviere
The Robotics Institute
Carnegie Mellon University
Pittsburgh, Pennsylvania, USA
camr@ri.cmu.edu

ABSTRACT
We describe early efforts in design and development of an In-Loop Electromagnetic Tracker (ILEMT), designed to meet the demanding latency and resolution requirements for handheld robotic systems that perform active stabilization of hand motion during microsurgery. The objective is to surpass the best commercial electromagnetic trackers in latency while matching them in root-bandwidth/resolution. The concept is to use frequency-domain multiplexing for fast measurementand high accuracy during rapid motion, and bifrequency dual-path eddy-current compensation(reducing distortion from metals without sacrificing speed). The use of two widely spaced carrier frequencies (e.g., 300 Hz and 10 kHz) enables a particularly simple way of reducing the eddy-current interference caused by nonferrous metals. Previously, metal compatibility has come at the price of reduced measurement speed.

CCS Concepts
• Computer systems organization→Robotics.

Keywords
medical robotics; sensors and applications; electromagnetic tracking; microsurgery; active error compensation

1. INTRODUCTION
Motion trackers measure the pose (position and orientation) of a freely moving object in six degrees of freedom (6DOF) using a sensor or tracking target attached to the object and external devices that establish a fixed reference frame. Trackers are widely used for surgical navigation and human motion capture. Optical tracking is most common; optics can be highly precise, and when only a 30-60 Hz measurement rate is needed, then sensing can be done using inexpensive video cameras. A main shortcoming of optical tracking is that it requires multiple sightlines to the tracker targets. Inertial tracking requires no sightlines, but can only track orientation and short-term relative motion, not absolute position [11]. Electromagnetic (EM) tracking requires no lines of sight, but is susceptible to interference due to other metallic objects in the workspace [8].

Routine clinical use of surgical robots has been hindered by size, difficulty of use, cost, and incompatibility with existing clinical workflow [7]. The demand for inexpensive and user-friendly systems is increasinginterest in handheld robotic instruments [9]. However, clinical usability of handheld robots is greatly impaired by the inadequacy of current trackers. Accurate tool tracking is essential for robot-assisted surgery,but available trackers are inadequate for microsurgery (Figure1): their resolution is too coarse [12], and their latency makes them fundamentally unsuited for use within the control loop, especially in handheld robotic instruments, where the control system must correctly track 1-20 Hz involuntary hand motion [2]. For the most demanding types of microsurgery (e.g., vitreoretinal), few suitable tracking systems exist, and none is commercially available [12].

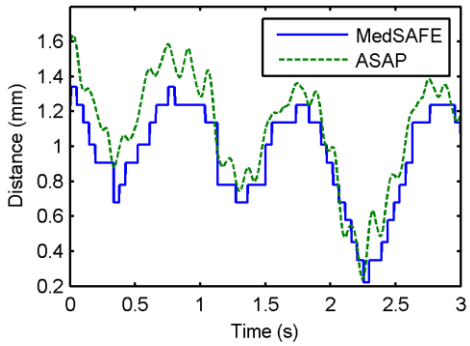

Figure1.Comparison of Ascension medSAFE™ electromagnetic tracker with our group's ASAP optical tracker loop. The latency or lag of medSAFE™ and its low precision and low bandwidth (note the discretized appearance of its data) are all evident in the plot.

We previously developed an optical tracker (Apparatus to Sense Accuracy of Position (ASAP)) [6] for use in Micron (Figure 2, foreground), a handheld instrument that performs active cancellation of hand tremor during microsurgery[5]. This use places extreme demands on measurement speed (latency) and resolution (noise). The effectiveness of active cancellation is fundamentally limited by delay [2]. Hand tremor contains significant energy at up to 10 Hz; to compensate 90% of this motion requires a total system latency of only a few milliseconds. Noise is also critical, since itcan be passed through to the tool motion. ASAP has acceptable speed and resolution, but it is difficult to use in surgery because of frequent sightline obstructions. As a result, our group has begun to design an In-

ICMRE '17, February 08-12, 2017, Paris, France

ACM ISBN 978-1-4503-5280-2/17/02...$15.00

DOI:http://dx.doi.org/10.1145/3068796.3068823

Loop Electromagnetic Tracker (ILEMT), with the low latency and high accuracy requisite for such an application.

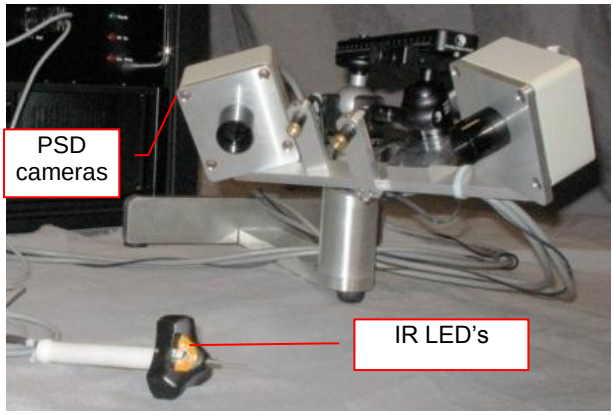

Figure2.Custom optical tracker (Apparatus to Sense Accuracy of Position (ASAP)).

2. METHODS

An electromagnetic (EM) tracker is an instrument that measures the position and orientation (or *pose*) of freely moving objects such as surgical instruments by using a small *sensor* attached to the object which detects the magnetic field emitted by a fixed *source.* Although source and sensor operation depend on electromagnetic induction, the reference field created by the source is effectively purely magnetic[10]. The magnetic field is a vector field, so at every point in space the field has both a direction and magnitude. When the source size is small compared to the operating distance it can be approximated as a point (a magnetic dipole). Figure 3 shows a 2D EM tracker that measures the 3DOF (r, θ, ϕ) pose of the sensor. In vector form, the dipole field is

$$\boldsymbol{B} = 10^{-7}\frac{1}{r^3}[3(\boldsymbol{m}\cdot\hat{\boldsymbol{r}})\hat{\boldsymbol{r}} - \boldsymbol{m}], \qquad (1)$$

where $\boldsymbol{m}$ is the magnetic moment of the source, a fixed vector representing its orientation and strength, and $\hat{\boldsymbol{r}}$ is the unit vector in the direction of $\boldsymbol{r}$. In this two-dimensional example, we replace $\boldsymbol{m}\cdot\hat{\boldsymbol{r}} = |\boldsymbol{m}|\cos\theta$ and factor out $|\boldsymbol{m}|$, giving

$$\boldsymbol{B} = 10^{-7}\frac{|\boldsymbol{m}|}{r^3}[3\cos\theta\,\hat{\boldsymbol{r}} - \hat{\boldsymbol{m}}] \qquad (2)$$

Let $\boldsymbol{M}_{\hat{\boldsymbol{r}}} \equiv 3\cos\theta\,\hat{\boldsymbol{r}} - \hat{\boldsymbol{m}}$. Then

$$\boldsymbol{B} = 10^{-7}\frac{|\boldsymbol{m}|}{r^3}\boldsymbol{M}_{\hat{\boldsymbol{r}}}. \qquad (3)$$

Along any given source radius, $|\boldsymbol{B}|$ varies as $1/r^3$ and the direction of $\boldsymbol{B}$ does not change. $\boldsymbol{M}_{\boldsymbol{r}}$ determines the variation of $\boldsymbol{B}$ when $|\boldsymbol{r}|$ is held constant. The orientation of the field follows ellipsoidal loops (shown as blue field lines in Figure 3). As well as determining the field direction, $3\cos\theta\,\hat{\boldsymbol{r}} - \hat{\boldsymbol{m}}$ also contributes a magnitude variation of 2:1. The sensor makes a vector measurement $\boldsymbol{v} = (v_x, v_y)$ of $\boldsymbol{B}_s$, with respect to its own Euclidean coordinates. Although $r \propto 1/\sqrt[3]{|\boldsymbol{v}|}$, and the direction of $\boldsymbol{v}$ contains information about (θ, ϕ), these are coupled, and a single vector measurement also does not yield enough information for a complete pose solution; the source must emit multiple independent fields (not shown) which are measured to find the pose. Although complex, especially in three dimensions, there are effective iterative and closed-form solutions to this problem[3]. Our concern here is with the ultimate limits of EM tracker performance with respect to bandwidth, noise and workspace size, which can be illustrated using this model.

2.1 Specifications

The Micron system operates by sensing the surgeon's hand tremor and then introducing an equal but opposite movement of its own tip in order to perform active compensation [5]. Figure 4 shows a theoretical upper bound on the effectiveness of any active compensation system that has latency. A system that aims to cancel 90% of a 10-Hz disturbance must have measurement latency less than 2 ms. This sets the latency specification of 1.5 ms.

Measurement noise (or resolution) is also critical in such a system—this noise is injected into the tool motion as a side-effect of compensation. The internal limiting membrane in the eye is about 10 μm thick, and is routinely manipulated in microsurgery. Gaussian peak-to-peak noise is six times the RMS noise, so this sets a requirement of 1 μm RMS noise for the tracker.

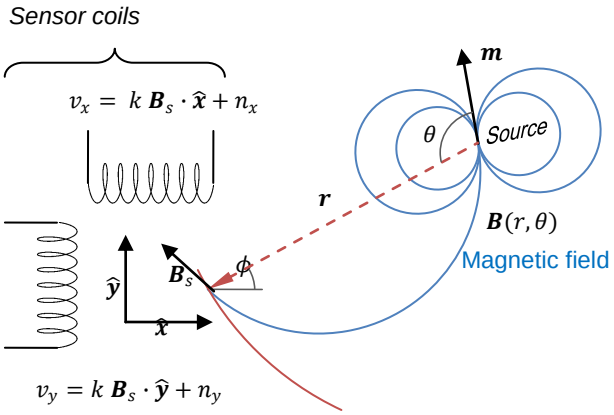

Figure 3.Simplified 2D EM tracker: a fixed source creates AC magnetic fields which sensor coils convert to a voltage v corrupted by noise n. Under a point-source approximation, v is easily determined when the sensor pose (r,θ,ϕ) is known, but the nonlinear inverse problem must be solved numerically. For a 6DOF solution, source and sensor need 3 coils each.

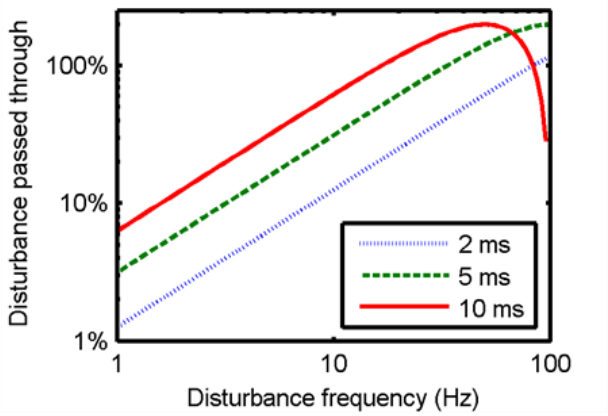

Figure 4.Disturbance sensitivity *vs.* total system latency (measurement + response).

2.2 Noise and Measurement Sensitivity

The sensor measurement is an analog voltage(v_x, v_y), corrupted by noise (n_x, n_y).Whether this noise is intrinsic to the sensor or from an external EM source, it will disturb the pose measurement. But $\boldsymbol{v}$ is a nonlinear function of the sensor pose (r, θ, ϕ), so we must determine the sensitivity of the pose solution to noise $\boldsymbol{n}$:

$$\boldsymbol{v} = k\,\boldsymbol{B_s} + \boldsymbol{n}, \tag{4}$$

where$k$ is the sensor gain. Substituting (3)for $\boldsymbol{B_s}$,

$$\boldsymbol{v} = k\,|\boldsymbol{m}|\,r^{-3}\boldsymbol{M_{\hat{r}}} + \boldsymbol{n}. \tag{5}$$

First, consider the sensitivity of r, which is determined primarily by $|\boldsymbol{v}|$. Since $|\boldsymbol{M_{\hat{r}}}|$does not depend on r, and varies only from 1 to 2, let $\boldsymbol{M_{\hat{r}}} = 1$, and differentiate (5) with respect to r:

$$\frac{d}{dr}|\boldsymbol{v}| \cong -3k|\boldsymbol{m}|r^{-4} \tag{6}$$

The error, Δr, due to $\boldsymbol{n}$ is then [8]

$$\Delta r \cong |\boldsymbol{n}|\left(\frac{d}{dr}|\boldsymbol{v}|\right)^{-1} \cong -\frac{r^4|\boldsymbol{n}|}{3k|\boldsymbol{m}|}. \tag{7}$$

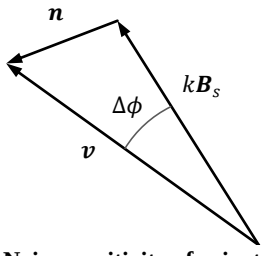

Figure 5.Noise sensitivity of orientation.

As for the sensitivity of (ϕ, θ), consider (4) as a vector addition, without regard to the sensor coordinates (Figure 5). Angle $\Delta\phi$ is small, so $\Delta\phi \cong |n|/(k|\boldsymbol{B}_s|)$. As before, we are only concerned with the magnitude of $\boldsymbol{B}$, so wecan set $\boldsymbol{M_{\hat{r}}} = 1$ when we substitute (3) for $\boldsymbol{B}_s$, giving

$$\Delta\phi \cong \frac{r^3|\boldsymbol{n}|}{k\,|\boldsymbol{m}|} \tag{8}$$

Comparing (7) and (8), note that angular noise does not increase as rapidly with r as does radial noise. Although we have used $\Delta\phi$ to refer to the angular deviation, this analysis applies equally to θ, which the pose solver also derives from field orientation at the sensor. The measurement in Figure 3 is fundamentally polar; hence the noise in the Euclidean position $\Delta\boldsymbol{x}$ is a composite of radial noise Δr and tangential noise $r\Delta\theta$. From (7) and (8), the ratio of tangential to radial noise is

$$\frac{r\Delta\theta}{\Delta r} = r\frac{r^3|\boldsymbol{n}|}{k\,|\boldsymbol{m}|}\left(\frac{3k|\boldsymbol{m}|}{r^4|\boldsymbol{n}|}\right) = 3 \tag{9}$$

So, allowing for the effect of polar measurement of position, the noise distribution of the Euclidean position has a fixed shape, dominated by tangential noise, and increases asr^4. Because of the dominance of tangential noise, $|\Delta\boldsymbol{x}| \cong r\Delta\theta$. Also, at a tool tip offset some distance r_t from the sensor, where $r_t \ll r$, then the translational noise $\Delta\boldsymbol{x}$will dominate the $r_t\Delta\phi$ contribution from angular noise. This inherently low angular noise is a desirable property of EM trackers.

2.3 AC *vs.* Pulsed-DC Modulation

The source must modulate to emit multiple reference vectors (multiplexing) and to allow the field to be distinguished from other interfering magnetic fields in the environment. In the AC approach, the source is driven with a sinusoidal carrier; in the pulsed-DC approach, an on/off pulse is used. The large low-frequency component in pulse modulation has important consequences for interference from metals (see below), but the pulsed-DC approach has fundamental limitations that prevent it from scaling to the noise levels and bandwidth required for handheld surgical robots. Most important, the broad spectrum of a pulse requires the sensor to have a broad noise bandwidth, several times the actual position measurement bandwidth. This increases the pulsed-DC tracker's susceptibility to sensor noise and 50/60 Hz electrical interference. In contrast, an AC tracker's noise bandwidth need only be as large as the measurement bandwidth, and is located well above power line frequencies. For this reason, our approach uses AC modulation.

2.4 Frequency-Domain Multiplexing

Another important advantage of sine modulation is that the source can emit the orthogonal reference fields simultaneously. Frequency-domain multiplexing (FDM) aidsrapid operation by allowing field measurements to be simultaneous, rather than switching a single carrier between axes[6]. This has a particular advantage when the measurement is highly dynamic, because measurement error is created when the sensor pose changes significantly during the time to takes to cycle between the three reference fields. Other causes may contribute, but existing trackers show significant increases in tracking error at frequencies as low as 9 Hz[1]. The principle of FDM reference fields has long been known[3], but it does not seem to be used in any current products. Likely this is because time-domain multiplexing is simpler, and is acceptable at current measurement rates. Significant increases in error during rapid motion often go

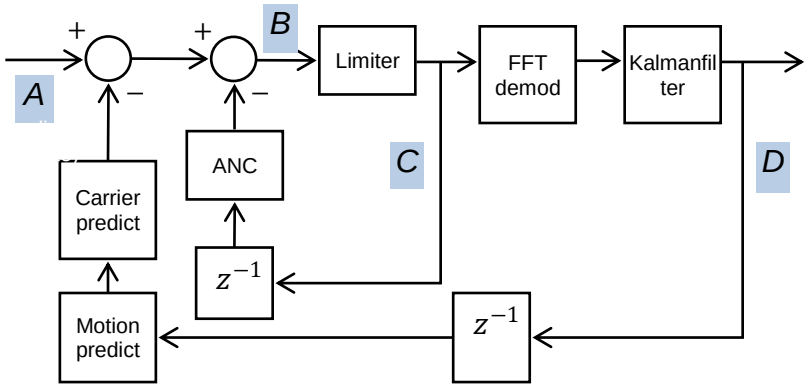

Figure 6.The ILEMT demodulator uses a Kalman filter, but the multi-rate structure puts the demodulator inside the feedback loop, computing prediction error (C) at the higher f_s rate input, enabling improved impulse rejection by the nonlinear limiter.

unnoticed by human observers, but robotic applications are more critical. Our approachtherefore uses FDM.

2.5 Metallic Interference

The main practical failing of EM trackersis that metal objects distort the source field[8]. *Eddy-current distortion* is an effect wherein changes in the source field (due to modulation) induce currents in conductive objects, which in turn create opposing magnetic fields. Highly conductive metals (Al, Cu) create larger distortion. Other metals such as stainless steel and titanium, commonly used in medical applications, have conductivity as much as 40 times less than aluminum, so the effect is smaller. Eddy currents are caused by the rate of change of the magnetic field, so are proportional to the modulation frequency. The 10-kHz (typical) carrier of an AC tracker is constantly changing, creating eddy-current distortion that can be significant even for low-conductivity metals. The leading edge of each pulse in a DC tracker induces significant eddy currents, but if the measurement is delayed until these decay (several milliseconds), the tracker can largely avoid eddy-current distortion, a significant benefit in medical applications. *Ferromagnetic distortion* is caused by materials such as steel which respond to external fields by creating an internal field thousands of times stronger, distorting the external field. This effect exists even for static fields, so all EM trackers are affected, but AC trackers are less susceptible because these metals are also conductive, and the eddy current fields oppose the ferromagnetic fields (reducing the effective permeability).

2.6 Electromagnetic Interference

Electromagnetic interference (EMI) from sources such as power lines also affects EM tracker performance. Existing EM trackers have notch and Kalman filters, but these filters add delay and other artifacts that are unacceptable in closed-loop use. Adaptive noise cancellation (ANC)[13] removes periodic EMI (e.g., hum) with no added latency by predicting and subtracting future noise. Other interference often takes the form of short impulses. These spikes are spectrally broad, so cannot be rejected by frequency-domain filtering. Aperiodic impulses (e.g., from switching) must also be rejected. Each EMI impulse affects only a few 10-µs input samples, but demodulation smears this interference across several 1-ms output samples. In the ILEMT Kalman demodulator (Figure **6**), a dynamic model sets configurable limits on acceleration and velocity. An impulse is inherently abrupt, but in microsurgery velocity rarely exceeds 10 mm/s, so motion during a 100-µs impulse must be less than 1 µm. Any larger apparent motion is unrealistic, and should be disregarded.

2.7 Test Apparatus

A 1DOF prototype has been constructed, incorporating the features described in the previous sections, as shown in Figure **6**. The prototype uses a USB audio interface (Steinberg UR44) to acquire the sensor signal and generate analog output for the source drivers. Because of buffering delays, this is not usable for real-time control, but the demodulation and EM interference rejection algorithms run at full rate in a PC LabVIEW application. Input is at 96k samples/s (approximately 20 bits resolution), and is demodulated using FFT blocks of 64 and 16K samples, with a window order of twice that length. This gives a high-rate bandwidth of 300 Hz; latency would be 1.3 ms with a one-sample processing delay. The high-rate output is 1500 samples/s, and the low-rate is 2× oversampled at 12 samples/s. The high carrier is 10.5 kHz. An audio amplifier module (IRAUDAMP7, International Rectifier) is used to drive 30V and 2.5A into the source coil, giving a source power dissipation of 3 W. This 75 VA output requires only 13 W of supplied power.

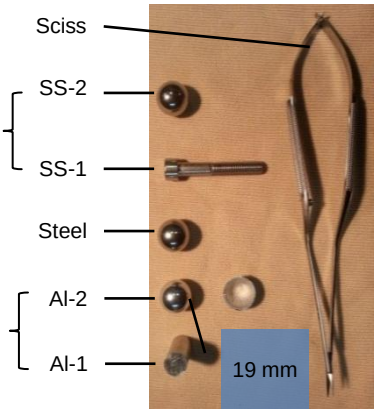

Figure 7.Test objects for metallic interference, placed between source and sensor at 50mm from sensor. Al-x aluminum, SS-x 18-8 stainless. Al-1, Al-2 are equal volume, but Al-2 is hollow (1mm wall). Sciss is a surgical micro-scissor.

2.8 Testing

The signal-to-noise ratio (SNR) of the field strength measurement was tested, and the responses of the low and high carriers were compared by tapping on the apparatus.To compare metallic interference at the different carrier frequencies, six metal test objects (Figure 7) were moved individually between the sensor and source. To assess the suppression of electromagnetic interference by the system, measurement corruption by impulse noise was generated artificially, and the output was recorded.

3. RESULTS

The SNR of the field strength measurement was measured at 100 dB at the full 1 kHz output rate. Figure 8 shows the relative responses of the two carriers to a tap on the apparatus.

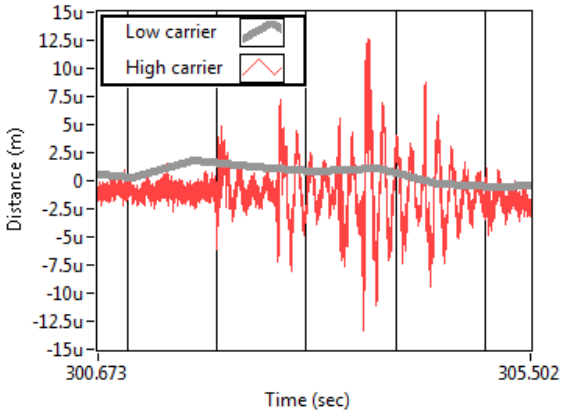

Figure 8.Response to a tap on the apparatus. High carrier captures 24-µm vibration near 8 Hz; low carrier only reflects gross motion.

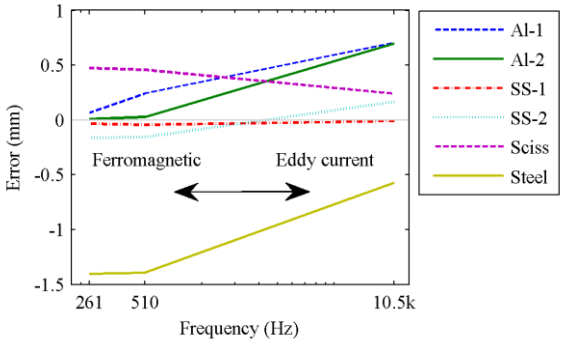

Figure 9.Position error due to metallic interference from objects in Figure 7. Non-ferromagnetic metals (Al) have least error at low frequency, and, if conductivity is low (SS-1), little error at all. Ferromagnetic effect is large at low frequency, but eddy current opposes this.

Figure 9 shows the position error of the ILEMT 1D prototype due to the metal test objects of Figure 7 at the different carrier frequencies. Eddy currents oppose the source field, and vary with frequency and conductivity according to the *skin depth*, the depth that induced fields permit the external field to penetrate. If the smallest dimension is more than twice the skin depth, current is confined to the surface, reducing interference. So for large high-conductivity objects, skin depth increases as frequency is reduced, current decreases more slowly, and interference reduction is less than the high/low ratio. At 10 kHz, skin depth is 2 mm for 6061 Al, where the effect of the hollow ball AL-2 is identical to the same-volume cylinder AL-1. At 510 Hz the 1-mm thickness of AL-2 is less than the skin depth, and eddy current interference disappears, while the solid AL-1 still creates significant error. Stainless steel object SS-1 has similar volume to SS-2, but is thinner than the 8.4 mm 10 kHz skin depth. Ferromagnetic materials generate internal magnetic fields that distort the external field, and decrease with frequency, since eddy currents oppose them. For *soft*ferromagnets (Steel), the source field is intensified, making the sensor appear closer, while *hard*ferromagnets (Sciss) resist external fields, increasing themeasurement. Carbon steel is a strong ferromagnet, but rarely used in surgery. Stainless steels vary in ferromagnetism. Pulsed-DC trackers use low frequencies, making them highly susceptible to ferromagnetic interference. ILEMT measures at multiple frequencies, so it can compensate for any metal by fitting a model to the frequency response; the wide carrier separation improves compensation [4].

Figures 10 and 11 present the system performance in the presence of electromagnetic impulse interference. Plots in Figure 10

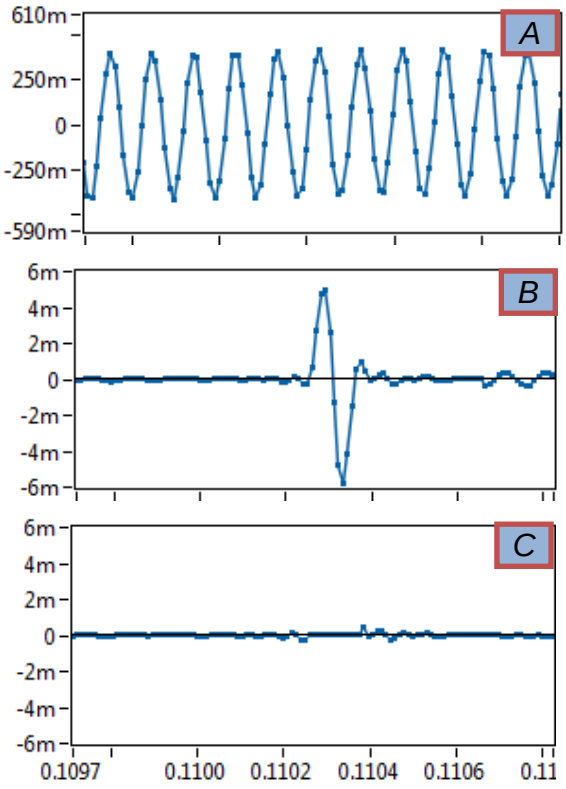

Figure 10.Performance in presence of impulse noise (plot labels correspond to markers in Figure 6). Carrier measurement corrupted by impulse noise (*A*), after carrier prediction and subtraction, impulse is clear (*B*), note vertical scale change; then pulse can be suppressed (*C*). Points mark individual f_s input samples. Impulse duration is 114 µs.

correspond to markers *A*, *B*, and *C* in Figure 6; Figure 11 corresponds to marker *D*.

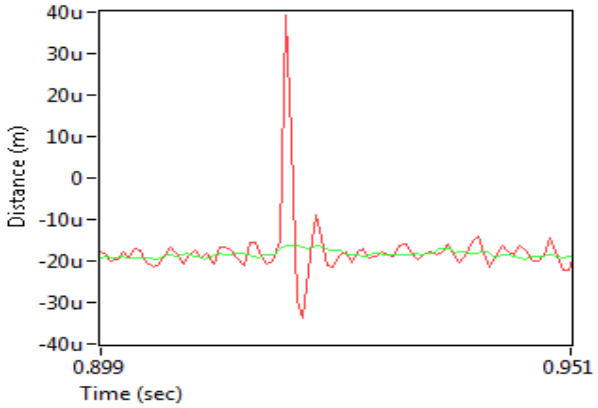

Figure 11.Impulse disturbance in measured distance at f_d = 1.5 kHz (Figure 6, *D*). With Kalman demodulation, effect is at the noise floor. Note different time scale and distance units (μm).

4. DISCUSSION

This paper describes preliminary design work toward a new in-loop EMT that improves on the speed and resolution of current EM trackers, while also maintaining the desirable rejection of eddy-current interference shown by pulsed-DC and other dual-frequency tracker designs. The possibility of using multi-sinedrive signals opens a wide range of options for compensation of metallic interference based on the different frequency responses of different disturbing objects. Until now, it has been necessary to trade off speed and resolution against eddy current interference rejection.

5. CONCLUSION

The combination of bifrequency dual-path eddy-current compensation with frequency-domain multiplexing may enable an EMT with accuracy and latency adequate for handheld microsurgical robotics. Research in this area is ongoing.

6. ACKNOWLEDGMENTS

Funding provided by the U.S. National Institutes of Health (grant no. R01EB000526).

7. REFERENCES

[1] Adelstein, B.D., Johnston, E.R. and Ellis, S.R. 1996. Dynamic response of electromagnetic spatial displacement trackers. *Presence*. 5, 3 (Jan. 1996), 302–18.

[2] Claasen, G.C., Martin, P. and Picard, F. 2011. Tracking and control for handheld surgery tools. *Proc IEEE Biomedical Circuits and Systems Conference (BioCAS)* (Nov. 2011), 428–431.

[3] Jones, H.R. 1985. Method and apparatus for determining remote object orientation and position. U.S. Patent 4,737,794, Apr. 12, 1988. 4737794. 1985.

[4] Khalfin, I. 2003. Method and apparatus for electromagnetic position and orientation tracking with distortion compensation employing modulated signal. U.S. Patent 6,624,626, Sept. 23, 2003. 2003.

[5] MacLachlan, R.A., Becker, B.C., Cuevas Tabares, J., Podnar, G., Lobes, Jr., L.A. and Riviere, C.N. 2012. Micron: an actively stabilized handheld tool for microsurgery. *IEEE Trans. Robot.* 28, 1 (2012), 195–212.

[6] MacLachlan, R.A. and Riviere, C.N. 2009. High-speed microscale optical tracking using digital frequency-domain multiplexing. *IEEE Trans. Instrum. Meas.* 58, 6 (Jun. 2009), 1991–2001.

[7] De Momi, E. and Ferrigno, G. 2010. Robotic and artificial intelligence for keyhole neurosurgery: the ROBOCAST project, a multi-modal autonomous path planner. *Proceedings of the Institution of Mechanical Engineers. Part H, Journal of engineering in medicine*. 224, (2010), 715–727.

[8] Nixon, M.A., McCallum, B.C., Fright, W.R. and Price, N.B. 1998. The effects of metals and interfering fields on electromagnetic trackers. *Presence*. 7, 2 (Apr. 1998), 204–218.

[9] Payne, C.J. and Yang, G.-Z. 2014. Hand-held medical robots. *Ann. Biomed. Eng.* 42, 8 (2014), 1594–605.

[10] Raab, F., Blood, E., Steiner, T. and Jones, H. 1979. Magnetic position and orientation tracking system. *IEEE Transactions on Aerospace and Electronic Systems*. AES-15, 5 (Sep. 1979), 709–718.

[11] Ren, H. and Kazanzides, P. 2012. Investigation of attitude tracking using an integrated inertial and magnetic navigation system for hand-held surgical instruments. *IEEE/ASME Trans Mechatron*. 17, 2 (2012), 210–7.

[12] Sznitman, R., Richa, R., Taylor, R.H., Jedynak, B. and Hager, G.D. 2013. Unified detection and tracking of instruments during retinal microsurgery. *IEEE Trans Pattern Anal Mach Intell*. 35, 5 (May 2013), 1263–73.

[13] Widrow, B., Glover, J.R., McCool, J.M., Kaunitz, J., Williams, C.S., Hearn, R.H., Zeidler, J.R., Dong Jr, E. and Goodlin, R.C. 1975. Adaptive noise cancelling: Principles and applications. *Proceedings of the IEEE*. 63, 12 (Dec. 1975), 1692–1716.